AIMS Geosciences

AIMS Geosciences, 11(1): 68–90.
DOI: 10.3934/geosci.2025005
Received: 29 November 2024
Revised: 11 February 2025
Accepted: 17 February 2025
Published: 24 February 2025

https://www.aimspress.com/journal/geosciences

Research article

Ries impact deposits in the North Alpine Foreland Basin of Germany as a terrestrial analog site for impact-produced seismites and sand spikes on planet Mars

Elmar Buchner[1,2,*], Volker J Sach[2,3] and Martin Schmieder[1,2]

[1] HNU, Neu-Ulm University of Applied Sciences, Wileystraße 1, D-89231 Neu-Ulm, Germany
[2] Meteorkrater-Museum Steinheim, D-89555 Steinheim am Albuch, Germany
[3] Fokus Natur, Am Heselsberg 29, D-88416 Ochsenhausen, Germany

*** Correspondence**: Email: elmar.buchner@hnu.de; Tel: +49 731 9762 1446.

Abstract: The North Alpine foreland basin (NAFB) in Germany is characterized by various types of sedimentologic features that make it an excellent terrestrial analog of regions affected by high-energy asteroid impact-quakes on Mars. Impact events have shaped all planetary bodies in the inner Solar System over the past >4 Gyr. The well-preserved Ries impact crater (Baden-Württemberg and Bavaria), formed around 14.8 Ma, has recently been linked to an earthquake-produced seismite horizon in Mid-Miocene NAFB sediments that exhibits typical dewatering structures and is associated with sand spikes, seismically produced pin-shaped pseudo-concretions. In this terrestrial setting, the sand spike tails systematically point away from the Ries crater. On its path across Gale Crater, the Mars rover Curiosity seems to have observed a similar seismite horizon in early Hesperian lacustrine deposits including clastic dikes, convolute bedding, and, likely, sand spikes. Their orientation suggests that the nearby Slagnos impact crater might be the seismic source for the formation of those seismites. The Ries impact–seismite deposits can be traced over a distance of more than 200 km from the source crater (northern Switzerland), which makes the NAFB an excellent terrestrial analog for similar deposits and their sedimentologic inventory within Gale Crater's lake deposits on Mars.

Keywords: Earth; Mars; seismicity; sand spikes; seismite; North Alpine foreland basin; Molasse; Gale Crater; Mars Curiosity Rover; earthquakes; asteroid impact; impact crater

1. Introduction

Through time, impact events have modified all planetary bodies in the inner Solar System. In this study, we present and discuss sedimentologic evidence of large-scale, high-energy impact-quakes on both Mars and Earth, which can thus be interpreted as analogs. On Earth, a seismite horizon produced by the Mid-Miocene Ries impact earthquake, exposed at several localities within the North Alpine foreland basin (NAFB), represents a textbook example of a terrestrial impact seismite [1,2]. The ~24 km diameter Nördlinger Ries in southern Germany is a well-preserved asteroid impact crater (Figure 1) that has been intensely investigated since the 1960s [3,4]. It has a well-constrained mid-Miocene $^{40}Ar/^{39}Ar$ age of 14.808 ± 0.038 Ma [5,6]. Proximal Ries impact ejecta occur in several varieties, including suevite [3,4], a type of melt-bearing impact breccia. Distal ejecta produced by this impact event occurs, in addition to the Central European tektites (moldavites) [3–5], as the coarse-grained distal Ries ejecta layer, a locally reworked horizon of sand, pebbles, cobbles, and boulders of predominantly Upper Jurassic limestone [1,2,7–9]. This horizon is a very distinct stratigraphic marker bed within Neogene Molasse sediments of the NAFB [5–9]. The Ries ejecta clasts were ballistically transported as far as 180 km, deposited, and preserved in those finer-grained siliciclastic sediments [1,2,7–12].

The Ries impact event caused intense regional-scale seismic effects in the NAFB deposits within a considerable distance from the Ries crater [1,2,8–12]. A distinct seismite unit recently discovered in the western and central part of the NAFB in southern Germany is characterized by various effects of soft-sediment deformation, such as large paleo-slumps, convolute bedding, ball-and-pillow and flame structures, and clastic dikes [1,2,12]. The seismite is unequivocally linked to the Ries event by its cap of distal ejecta including shatter-coned limestone fragments and shocked quartz grains [1,2,8,9,12] and detailed stratigraphic correlation using European land mammal zones (see Figure 2 in [15]). All of these features are consistent with their formation in a seismite produced during an intense paleoearthquake [1,2,8,12]. The seismite horizon in NAFB deposits was presumably produced by a magnitude MW ~8.5 earthquake following the Ries impact [13]. Outcrop-scale soft-sediment deformation occurred within a radial distance of ~40–210 km from the Ries crater [1,2,8–12,14].

So-called sand spikes [15] are often associated with the horizon of soft-sediment deformation and commonly occur in the basal portion of the seismite [1,2,8,12,15]. At all Molasse exposures investigated and reported in the literature, their occurrence is stratigraphically restricted to the seismite horizon that is identical in age to the Ries impact event. The horizon is stratigraphically situated within the final cycle of clastic sedimentation during the evolution of the North Alpine foreland basin in the mid-Miocene (Figure 1), dominated by fluviolacustrine sandy deposits [15,16]. They occur in a large variety of shapes, such as single, arrow- or obelisk-shaped individuals, and spike- or sill-shaped aggregates. In some outcrops, board- and ledge-like aggregates dominate and form parallel to the general layering of their host sands. The sand spikes often occur in several stacked layers, e.g., at the Untereichen sand and clay pit [8,12,15,16], approximately 85 km south of the Ries crater [15]. Sand spikes may have a bulbous head attached to an outward-thinning, tail-like protrusion. The bulbous head can be almost perfectly round or can have an outer cauliflower-like texture [15,16]. Some sand spikes have an obelisk-like shape without a pronounced bulbous head, and it appears that the specific shapes of the sand spikes tend to vary with outcrop (i.e., sand spikes with bulbous heads are predominantly found at Ochsenhausen, while obelisk-type sand spikes commonly occur at Untereichen and near Günzburg). Typical sand spikes from the NAFB mainly consist of quartz and, to a minor degree, feldspar, mica, and accessory minerals. Thus, they are essentially identical in modal composition and grain size with their host deposits [15–17]. The majority of sand spikes are cemented

by relatively pure calcite. The size of individual sand spikes ranges from a few centimeters to several tens of centimeters and, rarely, more than a meter [15–17]. Therefore, the size of sand spikes is not immediately diagnostic in the field.

Figure 1. Geographic and geologic situation in southern Germany, northern Switzerland, and Austria with the position of the Nördlinger Ries impact crater and the western and central part of the North Alpine foreland basin (NAFB). Red stars mark locations where the Ries seismite horizon crops out (many of them overlain by the distal Ries ejecta layer), and orange stars mark outcrops in the Ries seismite horizon mentioned in this study. Sand spike-bearing deposits are situated within a distance of up to ~140 km from the Ries crater; outcrops with deposits that exhibit convolute bedding, clastic dikes, and/or sand diapirs even occur within a distance of more than 200 km from the impact site (figure from [8,12,15], modified).

Sand spikes do not represent sand concretions [15], as was the common explanation for these peculiar, often times odd-shaped, calcite-cemented, sandstone bodies [15,17]. Rather, the outer appearance and the featureless inner texture of the sand spikes are consistent with their formation as sand injectites, a special form of a seismite [15]. Accordingly, sand spikes could be labeled *pseudo-concretions*.

At least 95% of the investigated sand spike tails from the NAFB point toward an SSW direction with a relatively small natural angular variance [15,17]. That is, the sand spike tails point away from the Nördlinger Ries crater, considered their seismic source, situated NNE from the sand spikes. This

systematic orientation of the sand spikes, together with their occurrence in direct association with the at least ~6–15 m thick Ries seismite layer, further supports the notion that they are genetically related to the Ries earthquake [15].

Sand spikes similar in shape, internal structure, and size to those from various localities in the NAFB were also found in late-Neogene to early-Quaternary sands at Mount Signal in the Imperial Valley of southern California [15,18]. Those sand spikes range in size from about 3 to 33 cm and also occur in a variety of shapes. Some come with heads that are perfectly round and spike tails that are long, tapering, or knobby. Some of the sand spikes exhibit cauliflower-textured heads, akin to those from the NAFB. Obelisk- and board-like specimens also occur. Over 95% of the spike tails at Mt. Signal point west [15,18] and appear to be genetically linked to the Imperial Fault as part of the long-term active San Andreas fault, a major fault system that lies some 35 km to the west [15,18]. This suggests that sand spikes at Mount Signal, which almost uniformly point away from the Imperial Fault, were generated during an episode of strong seismic shaking in that source region [15]. The earthquake strength induced by seismic activity or impact earthquake required to produce sand spikes is likely of an order of magnitude of MW ~7 or higher [15], which is in line with the strengths of historic earthquakes induced by the San Andreas fault system [19]. Additional possible sand spikes occur at various other localities on Earth, e.g., at the Ionian Coast, Italy [20] and Cape Liptrap, Victoria, Australia [21] (for a compilation of proposed sand spike occurrences, see [15]).

The discovery of sand spikes at terrestrial localities provides a clear idea of both the direction (azimuth) and distance of the (paleo-)seismic source that caused sand spike formation [15]. We posit that with high enough image resolution, sand spikes may also be recognized in sediments covering other water-bearing planetary bodies. In particular, planet Mars, on which large-scale seismites have been reported [22,23], represents a hot candidate for the presence of extraterrestrial sand spikes (ideally in association with other typical dewatering structures) in seismically disturbed sediments that were water-saturated or at least water-bearing during the "wet" late-Noachian and/or early-Hesperian time period [22,23]. If ever detected by one of the active Mars rovers, such as Curiosity, sand spikes on the red planet may indicate palaeoseismicity induced by larger meteorite impacts or seismic earthquakes in the past, at the same time offering estimates on the (past) volatile budget within the affected sediments. We investigated the relatively high-resolution photographs from the Mars Rover Curiosity [24], whose path leads across the ~3.5–3.7 billion-year-old (early-Hesperian), ~150 km diameter Gale Crater [22] and its (presumably fluviolacustrine) crater-fill deposits. In a systematic search for sand spikes and other sedimentary features typical of soft-sediment deformation on Mars, we explore whether palaeoseismic activity or impact-induced earthquakes could have produced seismites in Gale Crater's post-impact sediments, potentially comparable in stratigraphic anatomy and texture to those formed by the Ries impact earthquake in the NAFB in southern Germany [8,12,15]. The discovery of such features would have implications for the ongoing debate about the past water budget of early Mars.

2. Methods

2.1. Imagery from Mars Rover Curiosity

Mars Rover Curiosity was designed to explore the Gale Crater on Mars (Figure 2) as part of NASA's Mars Science Laboratory (MSL) mission [24,25]. It was launched from Cape Canaveral on November 26, 2011, and landed on Aeolis Palus inside Gale Crater on Mars on August 6, 2012 [24,25]. The rover is still operational, and as of 25 November 2024, Curiosity has been active on Mars for 4367

sols (more than 12 years) since its landing. The main mission goals include an investigation of the Martian climate and geology and whether the selected field site inside Gale Crater has ever offered environmental conditions favorable for microbial life, including an investigation of the role of (free) water. In our present study, we evaluated and interpreted raw and edited images combined into panoramic views. We evaluated images taken by Mars Rover Curiosity from sol 3050 and younger, when Curiosity entered the sedimentary cover of the Aeolis Mons area. A summary of online imagery resources is provided in Supplementary File S1. The size of image sections, sedimentological structures, and individual sedimentological features (such as clastic dikes or sand spikes) were gauged by comparing these features to the dimensions of the Mars Rover Curiosity. The information on the size of Martian image sections therefore contains certain margins of uncertainty. As sand spikes, clastic dikes, and associated sedimentary structures (e.g., convolute bedding) occur in a range of sizes and geometries in nature, we consider approximate size estimates for those features sufficient to support their geologic interpretation.

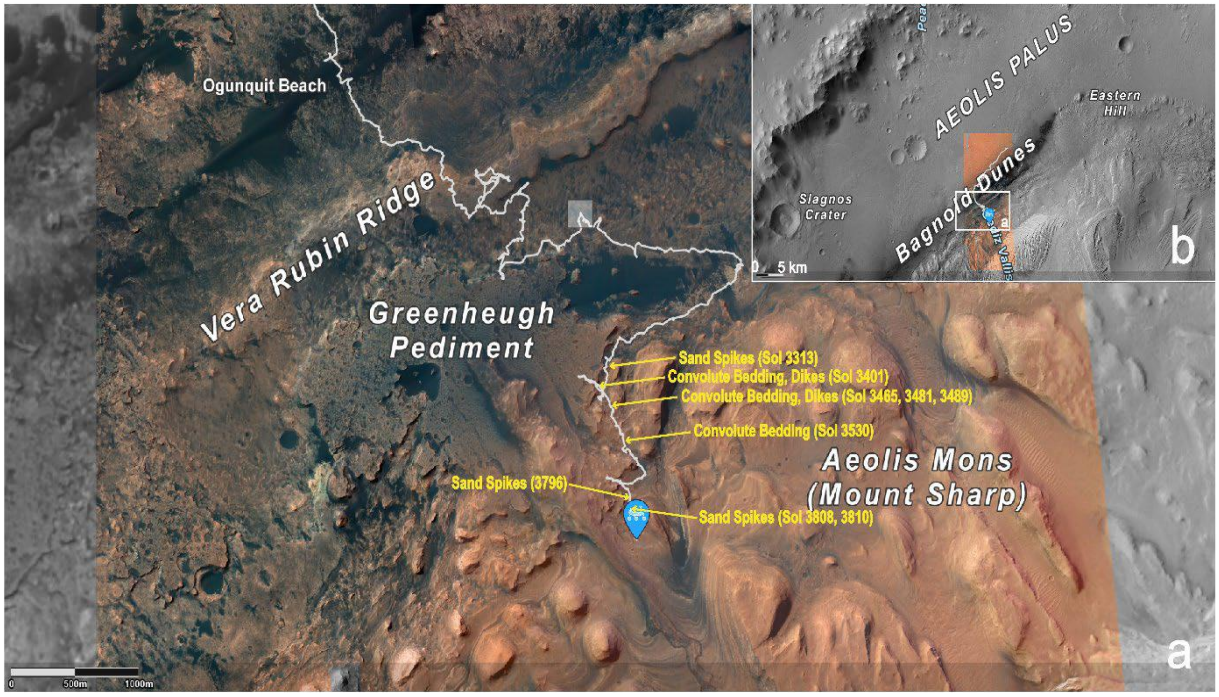

Figure 2. Mars Rover Curiosity inside Gale Crater. (a) Path of Mars Rover Curiosity within the ~150 km diameter Gale Crater. Curiosity entered Gale's central mound region (Mount Sharp) with fluviolacustrine deposits of Aeolis Mons end of 2021 around Solar Day (Sol) 3050. Locations along the rover's path with deposits showing the seismite horizon (including convolute bedding, sedimentary dikes, and/or sand spikes) within thinly layered lacustrine deposits are marked in yellow. (b) Position of the 6–7 km diameter Slagnos Crater in the Aeolis Palus [26–28] surface close to the northwestern crater rim in a zoomed-out map. Both images are from the NASA Mars Science Laboratory, Curiosity Rover, interactive map (https://science.nasa.gov/mission/msl-curiosity/location-map).

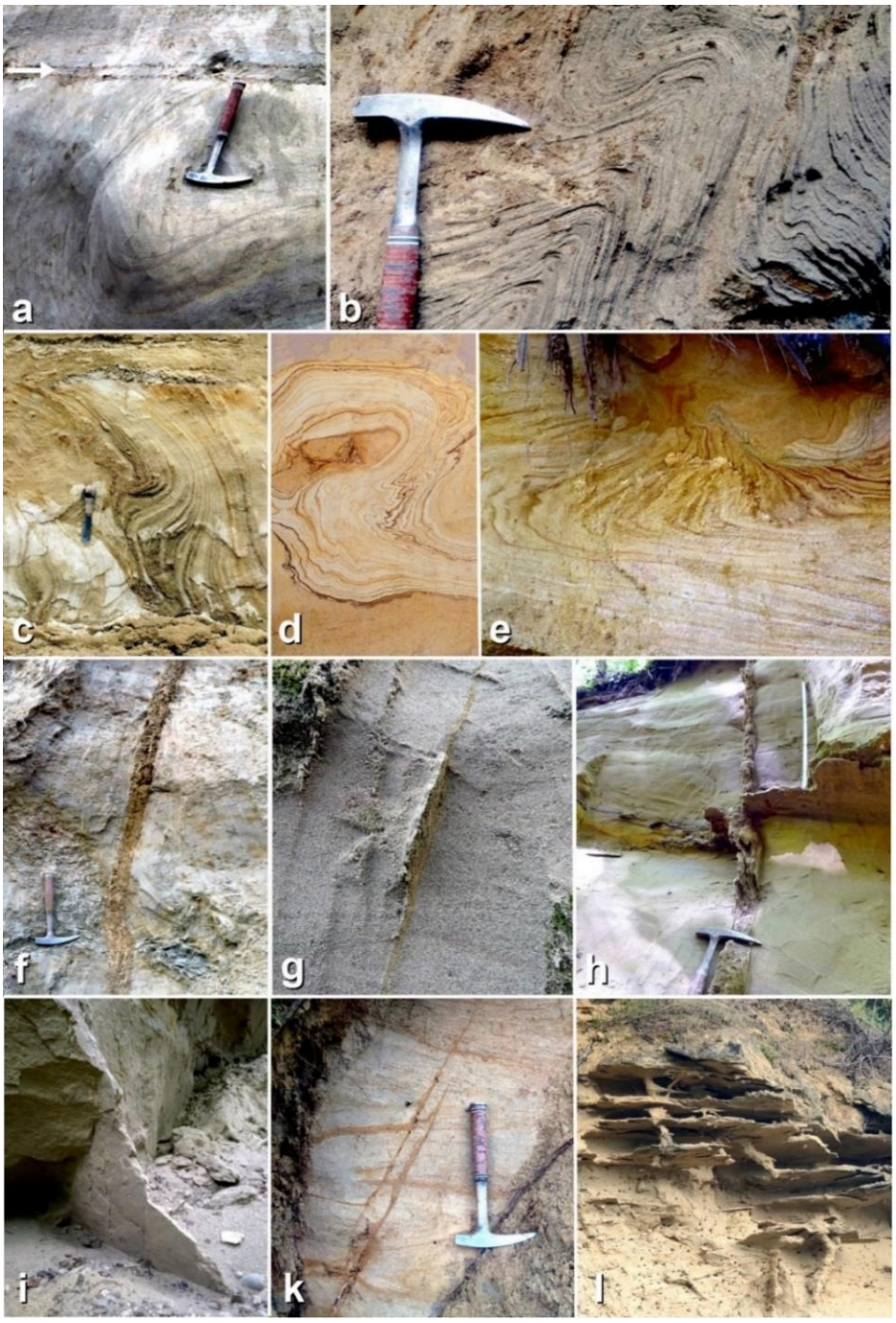

Figure 3. Dewatering structures showing slumps and/or convolute bedding (a–e) in NAFB deposits produced by the Ries impact earthquake. (a) Outcrop in the Kleintobel ravine close to Ravensburg, ~140 km SSW of the Ries crater. Sediments with folded bedding of slump structures are overlain by a horizon of distal Ries ejecta (hammer for scale). (b) Sediments showing convolute bedding in the outcrop Josefstobel (Hochgeländ, 100 km SSW of the Ries crater) with distinct folding and crumpling of the originally flat-lying strata (hammer for scale). (c and d) Convolute bedding in sediments of two temporary (summer 1995 and spring 2023) construction sites at Ochsenhausen (~90 km south of the Ries crater) close to Biberach an der Riß (width is ~2 m and ~1 m for c and d, respectively). (e) Convolute bedding in sediments of the Josefstobel ravine (width ~2 m). Clastic dikes and sills produced by the Ries impact earthquake (f–i) that crosscut NAFB deposits. (f and

g) Dikes in sediments of the Josefstobel and Kleintobel ravines near Biberach and Ravensburg, respectively; the fine-clastic infill of the dikes is laminated parallel to the dike walls and in places cemented by vertical layers or sheets of lamellar mineral precipitation (f, hammer for scale, g: width of scene is ~ 1 m). (h and i) Deposits in an outcrop in the Tobel Oelhalde-Nord ravine in the Hochgeländ plateau (~100 km SSW of the Ries crater), crosscut by a large clastic dike; the infill of the dike is laminated parallel to the dike walls and in places cemented by vertical layers or sheets of lamellar carbonate precipitation (h; hammer for scale) or mainly consists of lamellar carbonate precipitation (i; width of the scene is ~1.5 m). (k) Thin clastic dikes and sills that crosscut sandy molasse deposits in the Kleintobel ravine near Ravensburg (hammer for scale). (l) Clastic dikes and sills in the Untereichen sand and clay pit (width of the scene is ~2 m).

2.2. Geological field studies

In the last three decades (starting in 1993), natural outcrops, construction sites, and sand pits in Upper Freshwater Molasse deposits in the western and central part of the NAFB deposits were systematically investigated regarding their occurrence of seismite horizons (in the form of dewatering structures and clastic dikes and sills) and distal Ries ejecta (a detailed description of the sedimentologic inventory and outcrop coordinates is given in [2] and the supplementary file therein). In the last years, we expanded our investigations into those and other outcrops on the search for all kinds of dewatering structures including sand spike-hosting deposits produced by the Ries impact earthquake. In order to compare these terrestrial seismite structures to similar sedimentologic features in Aeolis Mons deposits on Mars, we paid particular attention to outcrops and ravines in the areas of Günzburg, Ochsenhausen, Dietenwengen, the Hochgeländ plateau south of Biberach an der Riß, and Ravensburg, all located in SW Germany. Sedimentary structures (in particular sand spikes, convolute bedding, dikes, and sills) in some of these outcrops were excavated (and reinvestigated) during several field campaigns in the summer of 2022 and, recently, in the spring and summer of 2023. We reinvestigated and newly excavated sandy deposits in the NAFB along the flanks of the “Tobel Oelhalde-Nord”, “Josefstobel” (Hochgeländ), and “Kleintobel” (Ravensburg). Further field investigations were carried out in active sand pits, in particular in the sand and clay pit Untereichen and in the sand and gravel pit near Dietenwengen.

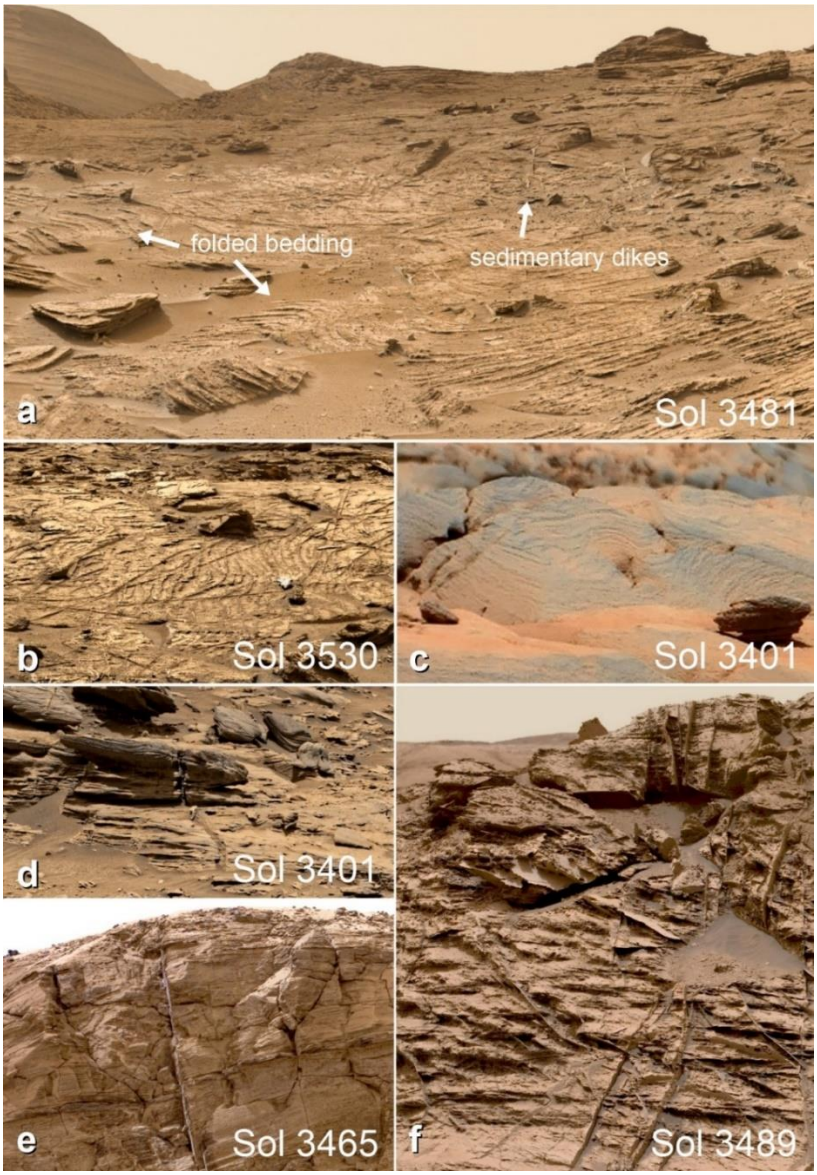

Figure 4. Convolute bedding and sedimentary (clastic) dikes in thinly layered deposits of Aeolis Mons. (a) Folded bedding in presumably lacustrine deposits, crosscut by some single small sedimentary dikes (estimated width of scene is ~8 m). (b) Folded and crumpled bedding of originally flat-lying strata, crosscut by likely sedimentary dikes; dikes and sedimentary deposits are shifted in places (estimated width of scene is 3–4 m). (c) Small-scale folded (convolute) bedding in lacustrine deposits (estimated width of scene is ~0.5 m). (d) At least two dikes crosscut the sedimentary deposits three-dimensionally; the dikes are distinct from the dike-hosting thinly layered deposits by their color and resilience (estimated width of the scene is ~2 m). (e) Sub-vertical and sub-horizontal likely clastic dikes in a butte exposure (estimated width of the scene is ~2 m). (f) Thin possible clastic dikes crosscut the thinly layered lacustrine deposits in various directions (estimated width of scene ~2.5 m). All raw images: NASA/JPL-Caltech/MSSS; panorama stitching and retouching by Andrew Bodrov (a), Neville Thompson (b, d, e), Todd (c), and Kevin M. Gill (f).

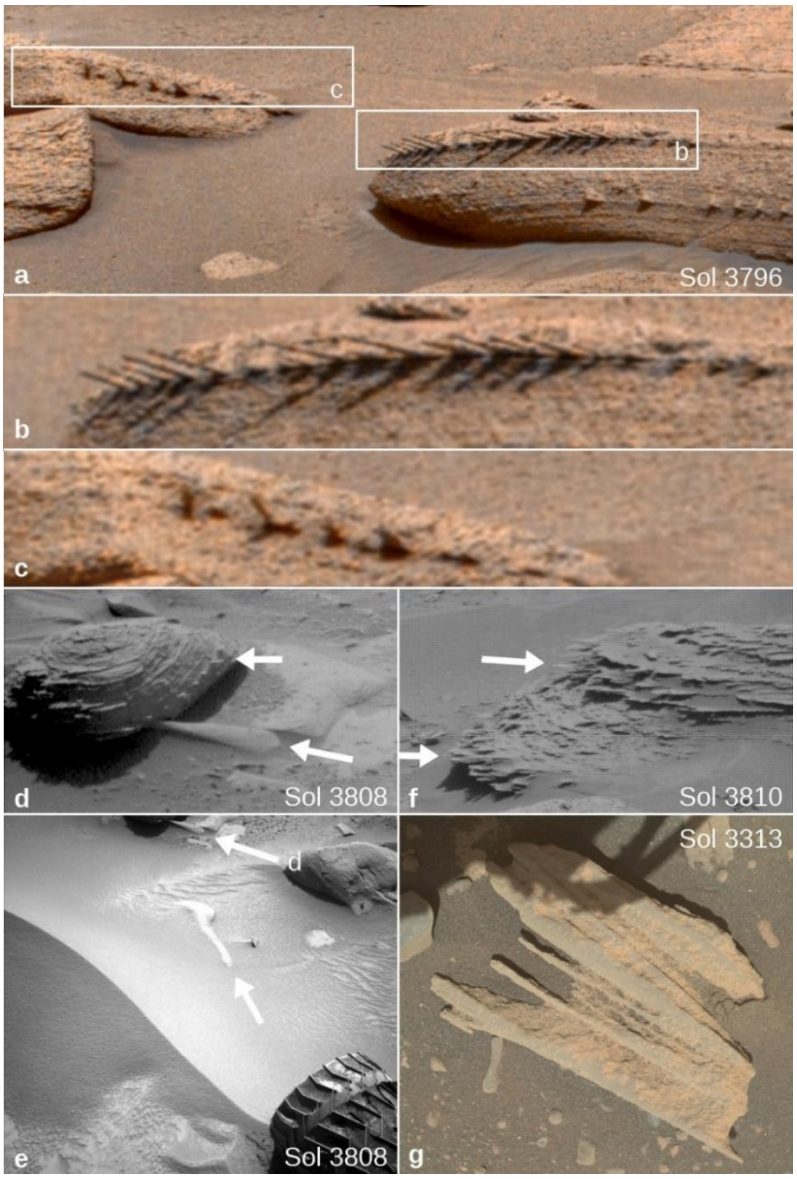

Figure 5. Sand spikes in different shapes in the thinly layered, lacustrine deposits of Aeolis Mons. (a, b, c) Board-like aggregates of sand spikes that formed parallel to the general layering of their host deposits; sand spikes arranged in a row strongly resemble fish-bones (estimated width of scene a is ~2.5 m and ~1 m for b and c). (d) Single obelisk-shaped sand spike specimen (lower arrow; width ~20 cm) and very small-scale board-like sand spike aggregate in thinly layered sandstone (upper arrow; estimated with of scene is ~0.6 m). (e) Obelisk-shaped sand spike (same as in d) and arrow-shaped sand spike in the center of the picture about 40 cm in length; width of rover wheel is ~40 cm. (f) Board-like, layered aggregates of sand spikes eroded from the thinly layered, lacustrine Aeolis Mons deposits; all sand spike apices point toward east (width of scene is ~2.5 m). (g) Elongated arrow-shaped sand-spikes weathered from the thinly layered lacustrine Aeolis Mons deposits (width of scene is ~0.6 m). All images: NASA/JPL-Caltech/MSSS.

3. Results

3.1. Post-impact deposits within Gale Crater

Mars Rover Curiosity was designed to explore the Gale Crater on Mars as part of NASA's Mars Science Laboratory (MSL) mission [24,25]. Mission goals encompass an investigation of the Martian climate and geology, including the role of water [24,25]. After the start of the Curiosity mission in August 2012 in the area of the Bagnold Dunes [26–28], the rover has more recently entered the area of Aeolis Mons (Mount Sharp) [26–28] in December 2021, i.e., around Solar Day (Sol) 3050. Sedimentary deposits within Gale Crater [26–29] (in particular in the Aeolis Mons area) include a ~90 m thick succession of thinly layered sedimentary rocks that, according to previous studies, probably formed in an ancient impact crater lake [26–29]. In the following 18 months, Curiosity delivered a large number of photographs [24] from different on-board cameras. A selection of specific sediment structures from the lacustrine or fluviolacustrine [28] deposits and their context will be described here in some detail.

3.2. Convolute bedding

This type of soft-sediment deformation describes originally water-bearing and unsolidified sedimentary beds disturbed by seismic waves induced by strong earthquakes [15,30]. Convolute lamination and deformation in unsolidified sedimentary deposits are usually found in fine or silty sands and may be confined to a specific water-saturated layer or to meter-thick water-bearing sections of the host strata (for some representative terrestrial examples of convolute bedding, see Figure 3a–e). Convolute bedding is often associated with other dewatering structures including sand blows (and sand volcanoes exposed at the former land surface) and sedimentary (clastic) dikes [15,31] (see Figure 3f–l for examples). We identified multiple scenes delivered by Curiosity showing convolute bedding (e.g., Sol 3401, 3481, 3530; Figure 4a, b, and c) in the thin-layered sedimentary deposits in the Aeolis Mons area, in particular in scenes taken on Sol 3400 and later [24]. Convolute bedding is particularly obvious in various scenes of Sol 3530–3531 [23], where complex folding, creasing, and crumpling of the originally flat-lying strata occurs. Thin, finer-grained, and obviously more solidified and competent deposits forming the layer boundaries clearly trace complex-folded bedding in the lacustrine deposits (Figure 4b). Likely sedimentary dikes [29,31] (for terrestrial examples, see Figure 3f–l; for Martian examples, see Figure 4a, b, and d–f) that crosscut the deposits with convolute bedding as well as sedimentary layers are locally displaced (Figure 4a, b). Characteristic wavy or flame-shaped deformation of thin-layered deposits of the Aeolian Mons region can be observed, for instance, near the center of the scene captured during Sol 3530 (Figure 4b).

3.3. Sedimentary dikes and sills

Clastic dikes (or sedimentary dikes) are more or less tabular bodies of clastic material (often fine sand to fine pebbles in grain size) that cut across sedimentary formations and typically exhibit (sub-)vertical lamination (Figure 3f–i). In unconsolidated sediments, clastic dikes form by the upward injection of a water-sediment mixture into overlying sedimentary bodies. Sedimentary dikes produced by earthquakes classified as seismites form by the injection of liquefied clastic material into (temporary) open fractures resulting from strong seismic shaking, simultaneously with fracture

propagation inside the host rock [30–33]. Locally, horizontal and/or vertical displacement (causing a visible offset) within the dike-hosting deposits can be observed (Figure 4b). The fine-clastic infill of the dikes is usually laminated parallel to the dike walls and in places cemented by also vertical layers or sheets (Figure 4e,f) of lamellar mineral precipitations of, e.g., phyllosilicates, secondary calcite, or sulfate minerals [1,8,9–11,15,30,31]. As discussed later, the cementation of the dikes and sheet-like lamellae by sulfates in the thinly layered deposits of Aeolis Mons is likely, as sulfates are the most common cement minerals in the sedimentary rocks of Gale Crater [28,34–36]. Those sheet-like mineral precipitates may stick out of the outcrop walls as a result of selective weathering [1,2,12] and may in places look similar (or even identical) to dike-like sulfate crack fillings unrelated to (seismic) soft-sediment deformation. Sedimentary dike structures are omnipresent features in the thinly layered sedimentary rocks of the Aeolis Mons area [24]. The dikes appear to be of sedimentary–seismic origin as they exhibit typical sedimentologic features for instance described for the Ries impact earthquake, which produced clastic dikes in the NAFB deposits [1,2,8–10,12,15], or clastic dikes associated with the Late Permian Araguainha impact in the Paraná Basin of Brazil [37], which also seem to have a similar appearance in length (up to several tens of meters) and width (typically millimeters to decimeters). The picture taken during Sol 3401 [24] exhibits at least two dikes that crosscut the sedimentary deposits three-dimensionally; the dikes are distinct from the dike-hosting thinly layered deposits by their color and petrovariance (i.e., resilience to weathering). The dike in the center of the photograph has an estimated length of ~1–2 m and a thickness of several centimeters, rendering it unlikely that this feature represents a secondary vein filling (which, however, cannot be entirely ruled out in the absence of compositional data; one has to note that clastic dikes can also be associated with and/or replaced by secondary fillings [37]). The infill of the dikes shown in various scenes of the rover's path through Aeolis Mons are laminated parallel to the dike walls and seem to be in places cemented by light-colored vertical layers of lamellar mineral coatings (e.g., Sol 3465). Many of these dikes are distinct from the dike-hosting deposits by their color, presumably in line with their (sulfate?) chemistry. Dikes and sills do not only crosscut the dike-hosting sediments but also crosscut each other (Sol 3489) in various directions. Magmatic dikes do not exhibit vertical, sheet-like lamellae and are usually more resistant to weathering than the surrounding rock, so that erosion exposes the dikes as natural walls or ridges. Taken together, the sedimentary characteristics mentioned above suggest that the dikes are best explained as clastic dikes rather than sand-filled cracks within the crater lake deposits.

3.4. Sand spikes

The formation of sand spikes [15] is a complex, polyphase process associated with the formation of other (classical) forms of seismites in the sense of dewatering structures (e.g., convolute bedding, clastic dikes) following the processes of seismically induced liquefaction and/or sediment dewatering. Sand spikes were recently identified to be a special type of a "wet" sand-derived seismite [15]. The spectrum of the appearance of sand spikes includes single, spike-, arrow-, or obelisk-shaped specimens and board-like aggregates that formed parallel to the general layering of their host deposits [15–17]. Sand spikes may occur preferentially along layer boundaries at some terrestrial outcrops in the NAFB [15], which suggests they form in basically dry sand bodies that still contain some fluid in layers or pockets. In the Aeolis Mons area on Mars, most of the sand spikes, probably cemented by sulfates (see discussion [28,34–36]), occur as board-like aggregates (Sols 3582, 3797, 3786, 3810) (Figure 5a–g). Such aggregates in the terrestrial NAFB deposits (e.g., sand and clay pit Untereichen [8,15,16]; Figure

6a–e) and in Martian deposits in Aeolis Mons area [28,29] (e.g., Sol 3796) are commonly lined up in a *fishbone pattern* along the general layering of the host deposits, and individual board-shaped aggregates (typically decimeters up to about 1 m in length) protrude from the layered sediment, thereby generating the impression of stick-like sand spikes (Figure 5). Those fishbone-shaped sandstone formations (i.e., Sol 7396) have provoked strange interpretations, including fossil dinosaur bones or fish skeletons, in popular scientific forums and associated social media. Locally, features strongly reminiscent of sand spikes (Figure 5d) weather out from their host deposits (Figure 6c). The dimensions of the sand spikes on Mars can only be estimated by comparing their length to the size of Mars Rover's wheels [24,25], which are approximately 40 cm in width [24]. We conclude that the length of the sand spikes observed in the area of Aeolis Mons ranges from ~20 cm for single obelisk-like specimens to roughly 1 m in the case of the board-like sand spikes. Hence, this size range is comparable to the average size of 20–30 cm in length of sand spikes from terrestrial occurrences [15]. Many of the sand spikes observed in Aeolis Mons area occur in slumped blocks of thin-layered sediments, and the orientation of the spikes and host rock layering significantly varies on a single scene (e.g., Sol 3786). However, in some scenes, sand spikes obviously occur within their host sediment in situ and all sand spikes (dozens of individuals) point toward the East (Sol 3810) when compared to Curiosity's southward travel route in the considered region [24] (Figure 2). In terrestrial environments with sand spike-bearing sediments (e.g., NAFB [15,17], Germany and Mount Signal, California, USA [15,18]), more than 95% of the sand spikes' apices point away from the seismic source inducing the seismic waves that formed the sand spikes. Assuming the formation mechanism for terrestrial sand spikes also applies on Mars, the seismic source responsible for the formation of the sand spikes should be situated somewhere west of the area of Aeolis Mons. In some image scenes, convolute bedding, crosscutting dikes, and sand spikes are spatially and stratigraphically associated. In all cases, sediments showing convolute bedding seem to overlie the sand spike-bearing deposits (e.g., Sols 3474, 3530–3531, 3401–3409, and, in particular, 3485–3520).

Figure 6. Sand spikes produced by the Ries impact earthquake in different shapes in thinly layered fluviolacustrine deposits of the NAFB. (a and b) Board-like, layered aggregates of sand spikes that formed parallel to the general layering of their host deposits from the Untereichen sand and clay pit; sand spikes arranged in a row strongly resemble fishbones; compare with Figure 5a, b, and c (width of scene a is ~4 m and scene b is ~0.6 m). (c) Obelisk-shaped single sand spike from a former sand pit close to Günzburg.; compare with Figure 5d (length of the sand spike is ~20 cm). (d) Board-shaped fishbone-like aggregates of sand spikes in the Josefstobel ravine in the Hochgeländ plateau (hammer for scale). (e) Board-like and arrow-shaped aggregates of sand spikes in the finely layered sandy deposits of the Untereichen sand and clay pit (width of the scene is ~3 m).

4. Discussion and conclusions

4.1. Characteristics of the Ries-produced seismite horizon in the NAFB

The dynamic process of seismite formation (including sand spikes) in the mid-Miocene NAFB sediments requires water-saturated or at least water-bearing unsolidified sandy deposits, which were

affected by a train of strong seismic waves (i.e., P-, S-, Love, and Rayleigh waves) sent out by the Ries impact [1,2,12,15,30,31]. Liquefaction of water-saturated loose sands in the NAFB sediments by earthquake-induced increasing pore pressure led to a vertical or horizontal flow of the liquefied sediment and the formation of characteristic dewatering structures such as convolute bedding and sand diapirs, visible in many outcrops in the western part of the NAFB [1,2,8–11,15]. Additional structural features of the seismite are clastic dikes and sills that form by the rapid and dynamic filling of temporary open fractures within the host sands [15]. Pore pressure increase was also responsible for the formation of sand spikes when the volume of liquefied sediment and, therewith, the difference in hydrostatic pressure between the liquefied sediment and the dry host deposits, was not sufficient to produce clastic dikes or sills [15]. The formation of dikes and sills by liquefaction of a sand–water mixture requires large, water-saturated sediment bodies [30,31]. The typical shape and relatively small size (up to 1 m) of the sand spikes, with roundish and/or cauliflower-like heads and tail-like protrusions that point away from the seismic source, suggest only small, water-filled pockets or limited water supply along layer boundaries in the host sands of the NAFB that burst upon seismic compression [15,17]. A mechanism referred to as "explosive flash vaporization" in earthquake-affected rocks [38] may have played a key role in sand spike formation. Fluids in the sediments affected by seismic pressure waves were decompressed to the point that water and other fluids turned into vapor after the passage of the fastest seismic wave, leading to decompression-induced flash vaporization [38]. Concomitant cavity expansion along faults, joints, layer boundaries, and/or other lithologic inhomogeneities within the sediment generated extreme reductions in pressure, facilitating a localized formation of pore fluid vapor. After explosive decompression and flash vaporization, portions of the affected sediment were absorbed into the transient cavities under temporary vacuum conditions [15,38]. The solubility of minerals (mainly calcite in the case of the terrestrial sand spikes) was strongly influenced by the chemical composition, pressure, and density of the fluid, and flash vaporization increased the degree of supersaturation by several orders of magnitude, resulting in the near-instantaneous precipitation of cement [15,38]. The rapid initial precipitation of calcite stabilized the sand spikes shortly after their formation, followed by intense and longer-lasting secondary calcification [15].

In the NAFB, sand spikes commonly show a preferred orientation along the pattern of the dewatering structures that point away from the Nördlinger Ries, the seismic source for the formation of sand spikes and the entire seismite horizon [15,17]. The Ries earthquake had an estimated moment magnitude of MW ~8.5 or somewhat higher [13,15], which means that sand spikes seem to form during very destructive earthquakes. Generally, a minimum moment magnitude of MW 5.5 is required for the formation of convolute bedding [30,31] and clastic dikes on the spot of their formation, and, most likely, at least MW 7 for the formation of sand spikes some tens of kilometers away from the hypocenter of the earthquake [15].

Sand spikes and more "classical" dewatering structures (clastic dikes, slumps, convolute bedding, flame structures, ball-and-pillow structures, and sand diapirs [1,2,12,30,31]) are often found together in one outcrop in the western part of the NAFB. The up to 15 m thick Ries seismite horizon [1,2,12,15] that formed within a radial distance of 40 km to considerably more than 100 km away from the seismic source [9–12,15] shows a certain internal stratification. The top of the seismite horizon is usually formed by slumps and sand diapirs, underlain by deposits showing convolute bedding, flame structures, and ball-and-pillow structures. Sand spikes typically occur within the basal parts of the seismite layers that are widely undisturbed or may show indistinct convolute bedding within the host sands surrounding the spikes [15]. Clastic dikes locally crosscut parts of or the entire succession of the seismite horizon [1,2,12,15], which may be an effect of protracted seismic shaking and deformation as

a sequence of seismic waves travels across the sediment body (with time gaps between the P-, S-, Love, and Rayleigh waves extending with increasing radial distance from the seismic source [15]).

Remote faulting of sedimentary deposits triggered by strong seismic waves far from the impact site was reported, for instance, from the Chicxulub asteroid impact at the Cretaceous–Paleogene boundary [32,33]. The distal formation of clastic dikes and sills on Earth far from the impact site was also described for various impact events [32,33,37]. In the Paraná Basin of Brazil, clastic dikes and sills occur within a distance of a few hundred to ~1,000 km away from the end-Permian Araguainha impact event [37]. Seismites produced by impact earthquakes are, however, particularly known from marine environments (e.g., seismite and/or tsunami units associated with the Chicxulub [32,33], Araguainha [37], and Manicouagan [39] impact events). The Ries seismite horizon in the NAFB deposits currently represents the best preserved (and maybe the only), exposed, and described continental seismite horizon [1,2,12,15].

4.2. Characteristics of a suspected seismite horizon at Aeolis Mons

Gale Crater is a ~150 km diameter [27–29] complex impact structure with a central mound (Mount Sharp, Aeolis Mons) that represents a transitional feature between a central peak and peak ring [28,29]. The early-Hesperian impact structure (3.5–3.7 Ga) [28,29] was the landing site of the 2011 Mars Science Laboratory mission [24] and the target region of the entire mission of the Mars Rover Curiosity [24,27]. That rover detected various lithologies in Gale Crater including sedimentary units. The data delivered by Curiosity indicate substantial sedimentary infill of Gale Crater [27–29], with some post-impact materials derived from the crater rim domain. The overall sedimentary cover of the central mound of Aeolis Mons is made of flat-lying strata, >250 m in thickness [28]. Several hypotheses have been proposed to explain those sedimentary deposits in the past, but data from Mars Rover Curiosity only seem to support a fluvial, deltaic, lacustrine, and/or aeolian nature of those sediments [26–28,40].

The >250 m thick sedimentary cover of Aeolis Mons includes a ~90 m thick succession of generally flat-lying, thinly layered sedimentary rocks [28], the sedimentologic features of which are consistent with deposition in a lacustrine paleoenvironment that had possibly formed in an ancient impact crater lake [26–28]. The lacustrine sedimentary strata inside the Gale Crater resemble small-scale bedding sequences seen in sediments from lacustrine environments on Earth [41]. Representative occurrences of those strata were described in detail from the lowermost crater walls of a fresh crater situated between the Gale Crater rim and the Aeolis Mons region [28]. The thinly layered material probably directly overlies the crater basement rocks and likely represents the oldest crater infill. Thus, those post-impact sediments are likely only somewhat younger than the Gale impact event itself. Curiosity entered the aera of Aeolis Mons around Sol 3050 or even somewhat earlier [24]. Besides some photographs that show (aeolian) dune deposits (Sol 3645–3670), most photographs sent by the Mars rover exhibit the thinly layered deposits that can be observed since Sol 3050. All our examples of suggested seismite features are hosted in originally more or less flat-lying and thinly layered deposits of lacustrine origin. The deposits showing convolute bedding stem from Sol 3041 to 3530, sand spikes from Sol 3796 to 3810 (one from Sol 3313), and clastic dikes from Sol 3460 to 3465. Sedimentary (clastic) dikes observed by Mars Rover Curiosity were also identified at Yellowknife Bay at an earlier stage of the rover's path through Gale Crater [42]. The entire seismite horizon may total an estimated thickness of ~5–10 m. According to our observations in the rover imagery, sediments that contain sand spikes stratigraphically underlie the deposits that exhibit convolute bedding in

combination with clastic dikes. This is strikingly similar to the findings in outcrops in the seismite horizon in NAFB sediments, where sand spikes either occur within the lowermost parts of (or directly below) deposits with convolute bedding [15]. Seismite formation in the Aeolis Mons region obviously follows the same fundamental mechanisms as in the NAFB deposits, which include as ingredients poorly solidified or even unsolidified, fine-grained, and water-bearing sediments affected by strong seismic waves [15]. Satellite data (CRISM and THEMIS) for the Gale Crater infill suggest dioctahedral and trioctahedral phyllosilicates as the main type of cement and fillings, varying in composition by location [35,36].

Furthermore, some olivine-bearing materials are hydrated/hydroxylated [28] into serpentine-group minerals. High-resolution visible and shortwave infrared data included a widespread distribution of olivine (sometimes with pyroxene) within the bedrock, hydrated silicates present in both bedrock and sediments, and regional or temporal differences in water chemistry as evidenced by the presence of chloride and sulfate salts detected by the rover inside Gale Crater [34–36]. Kaolinite-serpentine-group phyllosilicates, hydrated silica, and other hydrated/hydroxylated phases were detected regionally at various localities within Gale Crater [25,35,36]. All those results indicate an alteration of the local rocks by interaction with water [35,36]. Dewatering and liquefaction of water-bearing sediments at shallow depth (i.e., close to the former Martian land surface) would have produced convolute bedding. Compression and quick decompression of liquefied sand/water mixture in isolated water pockets or within boundary layers may have induced the formation of sand spikes in the deeper parts of the sedimentary body, likely in the same way as observed in the terrestrial outcrops in the NAFB [1,2,12,15]. However, in contrast to the NAFB, where cements are predominantly calcite, the cementation of the Martian sand spikes at Aeolis Mons would have been dominated by hydrated sulfates that are prevalent there [34–36]. In some of the NAFB outcrops, we observed sand diapirs and sand volcanoes [1,2,12,14,15], for instance on the Hochgeländ plateau close to Biberach an der Riß [5,8,15] and outside the city of Winterthur [14,15] in northern Switzerland (fossil Miocene sand diapirs and sand volcanoes locally known as the “Chöpfi” [14]). The formation of these sedimentologic features requires water-saturated sediment layers, liquefied to water/sand mixture rising up close to or entirely to the former land surface. In the thinly layered Aeolis Mons deposits [28], we did not observe any features that resemble fossil sand diapirs or sand volcanoes (albeit the latter are rare seismic features even on Earth), which may suggest Gale’s lake deposits were water-bearing rather than water-saturated at the time of the seismite formation. Some of the image scenes delivered by the Mars Rover Curiosity illustrate that the seismite horizon in Gale’s Crater lake deposits are overlain by additional thinly layered lacustrine deposits. This suggests that a) the seismite-hosting sediments were not covered by open water from a crater lake during seismite formation, b) the formation of the lake deposits had not terminated but must have continued after seismite formation, and c) Gales Crater’s lake infill was deposited under considerable fluctuations of the lake’s water level.

4.3. Possible seismic sources

According to our findings in terrestrial environments with sand spike–bearing sediments and the associated seismic sources that induced the sand spike-forming earthquake (NAFB/Nördlinger Ries, Germany [15,17] and Mount Signal/Imperial (San Andreas) Fault, California, USA [15,18]), sand spikes occur within a distance of ~30 to ~140 km from the seismic source, i.e., a radial zone of ideal conditions for sand spike formation. The earthquake strength required to produce sand spikes is

estimated to have been of order magnitude MW ~7 or higher [15]. As all sand spike apices observed in situ in the Aeolis Mons region point east (e.g., Sol 3810), the potential seismic source that produced those sand spikes would likely be situated some ~30 km or more west of Curiosity's path. A candidate that seems to fulfill these requirements is the ~6–7 km in diameter Slagnos impact crater [27] (Figure 2), situated ~35 km west of the rover's recent travel route, close to the west-northwestern inner crater rim of the ~150 km diameter and 3.5–3.7 Ga Gale Crater. Since the time Gale Crater and its (fluviolacustrine) sedimentary infill formed, the area was shaken by many impact events of unknown age, among them the impact that created Slagnos Crater. That impact structure is surrounded by a seemingly well-preserved layered ejecta blanket with lobe-like ramparts and long runout flows [27], similar to the characteristics of the ejecta blanket surrounding the Nördlinger Ries impact crater [43] in southern Germany in many ways. The appearance of Slagnos' ejecta blanket strongly argues for the formation of the impact structure in a volatile- and fluid-rich paleoenvironment and thus, probably shortly after the formation of Gale Crater, potentially contemporaneous with the deposition of lacustrine crater-fill sediments in the early-Hesperian. The preserved sedimentologic record of geologic activity inside the Gale Crater includes the deposition of sediments within a paleolake covering the crater floor in the center of the crater (Aeolis Mons) and the evolution of geomorphic features and surfaces on Aeolis Palus [27] (northwestern part of the Gale Crater between Aeolis Mons and the crater rim). The bulk of water-driven geomorphic shaping associated with the evolution of the crater interior would have been confined to the early-Hesperian [44]. The formation age of the Slagnos Crater and Gale Crater's lake deposits cannot be determined exactly; however, the Slagnos impact into water-bearing sediments in the Aeolis Palus surface might be simultaneous with, or slightly postdate, the formation of the lacustrine deposits in the Aeolis Mons area [41].

The size of the Slagnos event, creating a ~6–7 km diameter impact crater, would have been sufficient to impart enough energy into the Martian crust to induce a magnitude MW 7 impact earthquake, which is required to form sand spikes at a given distance from the crater [13,15]. This type of impact could have been accomplished, for instance, by a projectile ~400 m in diameter and with the density of a stony meteorite (3000 kg/m^3), at an impact velocity of 17.5 km/s and an impact angle of 70° [13], assuming an iron meteorite as the asteroid that produced Slagnos Crater, with density (8000 kg/m^3) and size (~300 m in diameter) having to be adjusted for modeling purposes [13]. Following the Slagnos impact event, the resultant earthquake would have had a Richter magnitude ML 7.0, corresponding to a moment magnitude around ~MW 7.3 (Supplementary File in [8]) at a radial distance of 35 km from ground zero. That earthquake strength would have been sufficient to produce a seismite horizon including sand spikes in the Aeolis Mons area more than 3.5 billion years ago, examined today in natural outcrops by Mars Rover Curiosity. We are aware of the fact that, theoretically, any other seismic source (impact event or seismotectonic activity) could have been responsible for the formation of a seismite horizon in the Aeolis Mons crater lake deposits. However, from its geographical position west of Aeolis Mons and its distance of 35 km from the seismite horizon, as well as from its presumably early-Hesperian age [27,28], the Slagnos impact event is an excellent candidate with respect to the seismic source that produced a veritable seismite layer associated with sand spikes in Gale's crater-lake deposits.

4.4. Implications for the environment and climate conditions on early-Hesperian Mars

An impressive, up to ~15 m thick seismite horizon in mid-Miocene fluviolacustrine deposits of the NAFB produced by the Nördlinger Ries impact earthquake [1,2,12,15] comprises deposits with

characteristic sand spikes, overlain by deposits showing convolute bedding and crosscut by clastic dikes [1,2,12,15]. This horizon is currently the only known example of a well-preserved impact-seismite in a continental setting on Earth. A similar, complex seismite horizon of estimated 5–10 m in thickness, again with a basal sand spike–bearing unit overlain by deposits with convolute bedding, crosscut by clastic dikes, occurs in Martian lacustrine deposits of the Aeolis Mons region. We argue that the seismite unit may have been produced by the Slagnos impact event, as far as the paleodistance, bearing, seismic magnitude, orientation of sand spikes, and host sediment properties are concerned. The mid-Miocene Ries impact scenario with its distal sedimentologic effects in the form of an impact seismite horizon in the NAFB probably represents the best terrestrial analog of an early-Hesperian [22], likely impact-produced seismite on Mars.

The environmental conditions in and around Gale Crater on early-Hesperian Mars were presumably rather "continental". Those conditions entailed a fluviolacustrine depositional environment near the center of Gale Crater with unconsolidated sediments and free fluid-bearing sandy deposits, as well as fluids saturated in ions derived from mineral dissolutions (e.g., sulfate, chloride). Furthermore, climate conditions were suitable for the existence of liquid water that enabled the existence of a permanent impact crater lake. Based on our argumentation that the Slagnos impact event induced the seismite-producing impact earthquake, environmental requirements and seismic conditions at the early-Hesperian Gale Crater are in many ways similar to those of the mid-Miocene terrestrial Ries-NAFB analog. Comparable processes of asteroid-triggered impact earthquakes in a similar environment of unconsolidated and water-bearing lacustrine deposits close to the former land surface seem to have produced analog effects in the form of seismites characterized by convolute bedding, clastic dikes, and sand spikes, but on two different planets. However, each one of those sedimentary features should be observed and interpreted in their sedimentologic context to make a more convincing case (e.g., convolute bedding in combination with likely sand spikes and clastic dikes as opposed to dike-like crack fillings alone) when one has to rely on photogeology alone.

The sedimentologic characteristics of the seismite horizon (in particular the lack of sand diapirs and sand volcanoes) in the Aeolis Mons deposits suggest water-bearing but not water-saturated conditions during seismite formation (i.e., the substrate was probably "moist" rather than "wet"). The seismite horizon probably formed in deposits that were not necessarily covered by water. However, seismite-hosting deposits in the Aeolian Mons region are unconformably overlain by additional flat-lying and thinly layered lake deposits. In earlier descriptions of the lacustrine deposits of Gale Crater, disruptions in sedimentation in the crater lake were explained by a shoreline of the lake that receded away from the crater rim with time [26–28]. Alternatively, another proposed setting may have been an episodic lake the depth of which fluctuated repeatedly [28]. However, the observed crater lake deposits with a seismite horizon again capped by another sequence of undisturbed lake deposits are not in line with a crater lake's shoreline that steadily receded from the crater rim. Rather, that sedimentary record is evidence of sequential and abrupt changes in the Martian environment [44,45]. Interbedded hydrated/hydroxylated sedimentary units suggest changing environmental conditions during lake sediment deposition, perhaps in a drying or episodically dry lake [28]. According to our observations and interpretations, a fluctuating water level in Gale Crater's lake favors episodic lakes or, even more plausible, is consistent with a long-lived crater lake whose water level episodically fluctuated depending on changing climate conditions. The first descriptions of terrestrial sand spike occurrences, some as early as ~200 years ago, stem from relatively young Neogene to Quaternary deposits. The occurrence of sand spikes in early-Hesperian deposits of Aeolis Mons on planet Mars strongly suggests

that these seemingly fragile sediment structures can, under certain circumstances, survive more than three billion years.

Author contributions

E.B., V.J.S., and M.S. designed the study and interpreted the results. E.B. prepared the results and led the initial paper preparation. M.S. prepared the figures. Discovery and documentation of seismite horizons, distal Ries ejecta, and sand spikes in the field, including digital photography, was done by V.J.S.. Sedimentological, litho- and biostratigraphical interpretations of field data and of photographs delivered by Mars Rover Curiosity was carried out by E.B., V.J.S., and M.S.. All authors contributed to the writing and editing of the paper.

Acknowledgements

The authors are grateful to several owners (undisclosed as per their request) of the active sand pits in the western part of the North Alpine Foreland Basin (i.e., sand and clay pit Untereichen, sand and gravel pit Dietenwengen) that gave us approval to study the seismite horizon and sand spikes in detail. The comprehensive image repository of raw and processed Mars Rover Curiosity images by NASA/JPL-Caltech/MSSS is also greatly acknowledged; we specifically acknowledge the efforts made by Andrew Bodrov, Kevin M. Gill, Neville Thompson, and Gigapan user Todd for their work stitching and retouching raw NASA images into comprehensive Mars surface panoramas useful in "photo sedimentology". We would also like to thank two anonymous reviewers for their critical and constructive comments. E.B. acknowledges a grant (project 11050) by the Stifterverband für die Deutsche Wissenschaft (Dieter Schwarz Stiftung) and gratefully dedicates his work to Dieter Schwarz, Heilbronn (founder of the Dieter Schwarz Stiftung and honorable research patron), for the generous and long-term financial support of his scientific work.

Use of AI tools declaration

The authors declare they have not used Artificial Intelligence (AI) tools in the creation of this article.

Ethics statement

Ethical standards have been followed during this research, which did not include work with living subjects.

Data availability

Data will be available on demand.

Conflict of interest

The authors declare no conflict of interest.

References

1. Sach VJ, Buchner E, Schmieder M (2020) Enigmatic earthquake-generated large-scale clastic dyke in the Biberach area (SW Germany). *Sediment Geol* 398: 105571. https://doi.org/10.1016/j.sedgeo.2019.105571
2. Buchner E, Sach VJ, Schmieder M (2020) New discovery of two seismite horizons challenges the Ries–Steinheim double-impact theory. *Sci Rep* 10: 22143. https://doi.org/10.1038/s41598-020-79032-4
3. Stöffler D, Artemieva NA, Wünnemann K, et al. (2013) Ries crater and suevite revisited—Observations and modeling. Part I: Observations. *Meteorit Planet Sci* 48: 515–589. https://doi.org/10.1111/maps.12086
4. Artemieva NA, Wünnemann K, Krien F, et al. (2013) Ries crater and suevite revisited—Observations and modeling. Part II: Modeling. *Meteorit Planet Sci* 48: 590–627. https://doi.org/10.1111/maps.12085
5. Schmieder M, Kennedy T, Jourdan F, et al. (2018) A high-precision $^{40}Ar/^{39}Ar$ age for the Nördlinger Ries impact crater, Germany, and implications for the accurate dating of terrestrial impact events. *Geochim Cosmochim Acta* 220: 146–157. https://doi.org/10.1016/j.gca.2017.09.036
6. Schmieder M, Kennedy T, Jourdan F (2018) Response to comment on "A high-precision $^{40}Ar/^{39}Ar$ age for the Nördlinger Ries impact crater, Germany, and implications for the accurate dating of terrestrial impact events" by Schmieder et al. (Geochim. Cosmochim. Acta 220 (2018) 146–157). *Geochim Cosmochim Acta* 238: 602–605. https://doi.org/10.1016/j.gca.2018.07.025
7. Sach VJ (1999) Litho- und biostratigraphische Untersuchungen in der Oberen Süßwassermolasse des Landkreises Biberach an der Riß (Oberschwaben). *Stuttgarter Beitr Naturk B* 276: 1–167.
8. Sach VJ (2014) *Strahlenkalke (Shatter-Cones) aus dem Brockhorizont der Oberen Süßwassermolasse in Oberschwaben (Südwestdeutschland)—Fernauswürflinge des Nördlinger-Ries-Impaktes*, Pfeil Verlag, München, 1–17.
9. Hofmann B, Hofmann F (1992) An impactite horizon in the upper freshwater molasse in Eastern Switzerland: Distal Ries ejecta. *Eclogae Geol Helv* 85: 788–789.
10. Letsch D (2017) Diamictites and soft sediment deformation related to the Ries (ca. 14.9 Ma) meteorite impact: the "Blockhorizont" of Bernhardzell (Eastern Switzerland). *Int J Earth Sci* 107: 1379–1380. https://doi.org/10.1007/s00531-017-1542-1
11. Holm-Alwmark S, Alwmark C, Ferrière L, et al. (2021) Shocked quartz in distal ejecta from the Ries impact event (Germany) found at ~ 180 km distance, near Bernhardzell, eastern Switzerland. *Sci Rep* 11: 7438. https://doi.org/10.1038/s41598-021-86685-2
12. Buchner E, Sach VJ, Schmieder M (2022) Event- and biostratigraphic evidence for two independent Ries and Steinheim asteroid impacts in the Middle Miocene. *Sci Rep* 12: 18603. https://doi.org/10.1038/s41598-022-21409-8
13. Collins G, Melosh HJ, Marcus R (2005) Earth impact effects program: a web-based computer program for calculating the regional environmental consequences of a meteoroid impact on Earth. *Meteorit Planet Sci* 40: 817–840. https://doi.org/10.1111/j.1945-5100.2005.tb00157.x
14. Schmieder M, Sach VJ, Buchner E (2021) The Chöpfi pinnacles near Winterthur, Switzerland: Long-distance effects of the Ries impact-earthquake? *Int J Earth Sci* 111: 145–147. https://doi.org/10.1007/s00531-021-02082-0

15. Buchner E, Sach VJ, Schmieder M (2021) Sand spikes pinpoint powerful palaeoseismicity. *Nat Commun* 12: 6731. https://doi.org/10.1038/s41467-021-27061-6
16. Maurer H, Buchner E (2007) Rekonstruktion fluvialer Systeme der Oberen Süßwassermolasse im Nordalpinen Vorlandbecken SW-Deutschlands. *German J Geosci (ZdGG)* 158: 249–270. https://doi.org/10.1127/1860-1804/2007/0158-0249
17. Heider J, Wegele A, Amstutz GC (1976) Beobachtungen über Sandrosen und Zapfensande aus der Süßwassermolasse Südwürttembergs. *Der Aufschluß* 27: 297–307.
18. Sanborn WB (1976) Oddities of the Mineral World. Van Nostrand Reinhold Company, NY, USA. 142. Available from: http://allanmccollum.net/amcimages/sanborn.html, (last accessed February 19, 2025).
19. Akçiz SO, Grant Ludwig L, Arrowsmith JR, et al. (2010) Century-long average time intervals between earthquake ruptures of the San Andreas fault in the Carrizo Plain, California. *Geology* 38: 787–790. https://doi.org/10.1130/G30995.1
20. McBride EF, Picard MD, Folk RL (1994) Orientated Concretions, Ionian Coast, Italy: Evidence of Groundwater flow direction. *J Sediment Res* A64: 535–540. https://doi.org/10.1306/D4267DFC-2B26-11D7-8648000102C1865D
21. McCullough LN, Ritter JB, Zaleha MJ, et al. (2003) Habit, formation, and implications of elongeate, calcite concretions, Victoria, Australia. Department of Geology, Wittenberg University, Ohio, USA. Published Senior Honors Thesis. 25.
22. Grant JA, Wilson SA (2018) Possible Geomorphic and Crater Density Evidence for Late Aqueous Activity in Gale Crater. LPI Contrib. 49th Annual Lunar and Planetary Science Conference.
23. Metz J, Grotzinger J, Okubo C, et al. (2010) Thin-skinned deformation of sedimentary rocks in Valles Marineris, Mars. *J Geophys Res Planets* 115: E11004. https://doi.org/10.1029/2010JE003593
24. NASA Mars Science Laboratory, Curiosity Rover, 2024. Available from: https://mars.nasa.gov/msl/mission/science/.
25. Wray JJ (2013) Gale Crater: The Mars Science Laboratory/Curiosity rover landing site. *Int J Astrobiol* 12: 25–38. https://doi.org/10.1017/S1473550412000328
26. Grotzinger JP, Sumner DY, Kah LC, et al. (2014) A habitable fluvio-lacustrine environment at Yellowknife Bay, Gale Crater, Mars. *Science* 343: 6169. https://doi.org/10.1126/science.1242777
27. Grotzinger JP, Gupta S, Malin MC, et al. (2015) Deposition, exhumation, and paleoclimate of an ancient lake deposit, Gale Crater, Mars. *Science* 350: 6257. https://doi.org/10.1126/science.aac7575
28. Buz J, Ehlmann BL, Pan L, et al. (2017) Mineralogy and stratigraphy of the Gale crater rim, wall, and floor units. *J Geophys Res Planets* 122: 1090–1118. https://doi.org/10.1002/2016JE005163
29. Schwenzer SP, Abramov O, Allen CC, et al. (2012) Gale Crater: Formation and post-impact hydrous environments. *Planet Space Sci* 70: 84–95. https://doi.org/10.1016/j.pss.2012.05.014
30. Montenat C, Barrier P, Ott d'Estevou P, et al. (2007) Seismites: An attempt at critical analysis and classification. *Sediment Geol* 196: 5–30. https://doi.org/10.1016/j.sedgeo.2006.08.004
31. Hargitai H, Levi T (2015) Clastic dikes, *Encyclopedia of Planetary Landforms*, Hargitai H and Kereszturi A, Eds., Encyclopedia of Planetary Landforms, Springer, NY, USA.
32. Sleep NH, Olds EP (2018) Remote faulting triggered by strong seismic waves from the Cretaceous-Paleogene asteroid impact. *Seismol Res Lett* 89: 570–576. https://doi.org/10.1785/0220170223

33. DePalma RA, Smit J, Burnham DA, et al. (2019) A seismically induced onshore surge deposit at the K-Pg. boundary, North Dakota. *PNAS* 116: 8190–8199. https://doi.org/10.1073/pnas.1817407116
34. Vaniman DT, Bish DL, Ming DW, et al. (2014) Mineralogy of a mudstone at Yellowknife Bay, Gale Crater, Mars. *Science* 343: 6169. https://doi.org/10.1126/science.1243480
35. Ehlmann BL, Buz J (2015) Mineralogy and fluvial history of the watersheds of Gale, Knobel, and Sharp craters: A regional context for MSL Curiosity's exploration. *Geophys Res Lett* 42: 264–273. https://doi.org/10.1002/2014GL062553
36. Carter J, Viviano-Beck C, Loizeau D, et al. (2015) Orbital detection and implications of akaganéite on Mars. *Icarus* 253: 296–310. https://doi.org/10.1016/j.icarus.2015.01.020
37. Tohver E, Schmieder M, Lana C, et al. (2018) End-Permian impactogenic earthquake and tsunami deposits in the intracratonic Paraná Basin of Brazil. *GSA Bull* 130: 1099–1120. https://doi.org/10.1130/B31626.1
38. Weatherley DK, Henley RW (2013) Flash vaporization during earthquakes evidenced by gold deposits. *Nature Geosci* 6: 294–298. https://doi.org/10.1038/ngeo1759
39. Simms JM (2003) Uniquely extensive seismite from the latest Triassic of the United Kingdom: evidence for bolide impact? *Geology* 31: 557–560. https://doi.org/10.1130/0091-7613(2003)031<0557:UESFTL>2.0.CO;2
40. Banham SG, Gupta S, Rubin DM, et al. (2018) Ancient Martian aeolian processes and palaeomorphology reconstructed from the Stimson formation on the lower slope of Aeolis Mons, Gale crater, Mars. *Sedimentology* 65: 993–1042. https://doi.org/10.1111/sed.12469
41. Bohacs KM, Carrol AR, Neal JE (2003) Lessons from large lake systems—Thresholds, nonlinearity, and strange attractors. *Special Papers-Geological Society of America*, 75–90. https://doi.org/10.1130/0-8137-2370-1.75
42. Brož P, Oehler D, Mazzini A, et al. (2023) An overview of sedimentary volcanism on Mars. *Earth Surf Dynam* 11: 633–661. https://doi.org/10.5194/egusphere-2022-1458
43. Sturm S, Wulf G, Jung D, et al. (2013) The Ries impact, a double-layer rampart crater on Earth. *Geology* 41: 531–534. https://doi.org/10.1130/G33934.1
44. Wilson SA, Morgan AM, Howard AD, et al. (2021) The global distribution of craters with alluvial fans and deltas on Mars. *Geophys Res Lett* 48: e2020GL091653. https://doi.org/10.1029/2020GL091653
45. Grotzinger JP, Crisp J, Vasavada AR, et al. (2012) Mars Science Laboratory mission and science investigation. *Space Sci Rev* 170: 5–56. https://doi.org/10.1007/s11214-012-9892-2

Supplementary file S1—Mars Curiosity Rover image resources

The map of Gale Crater shown in Figure 2 is available at: https://science.nasa.gov/mission/msl-curiosity/location-map.

Panorama-stitched and edited/retouched Curiosity images used in Figure 4:

a: https://www.360cities.net/image/mars-panorama-curiosity-solar-day-3481, panorama and retouching by Andrew Bodrov;

b: http://www.gigapan.com/gigapans/230023, panorama and retouching by Neville Thompson;

c: https://gigapan.com/gigapans/230449, panorama and retouching by Gigapan user Todd;

d: http://gigapan.com/gigapans/228756, panorama and retouching by Neville Thompson;

e: http://www.gigapan.com/gigapans/229328, panorama and retouching by Neville Thompson;

f: https://www.flickr.com/photos/kevinmgill/52114402597, panorama and retouching by Kevin M. Gill.

Raw Curiosity images used in Figure 5 are available online at: https://mars.nasa.gov/msl/multimedia/raw-images/?order=sol+desc%2Cinstrument_sort+asc%2Csample_type_sort+asc%2C+date_taken+desc&per_page=50&page=0&mission=msl.

Detailed information about the dimensions of the Mars Rover Curiosity is available at: https://mars.nasa.gov/msl/spacecraft/rover/summary/.